

<https://doi.org/10.1038/s42003-024-06314-2>

Nesfatin-1 and nesfatin-1-like peptide attenuate hepatocyte lipid accumulation and nucleobindin-1 disruption modulates lipid metabolic pathways

Atefeh Nasri¹, Mateh Kowaluk¹, Scott B. Widenmaier² & Suraj Unniappan¹

Nesfatin-1 (NESF-1) has been shown to modulate lipid metabolism. We have identified a nesfatin-1-like-peptide (NLP) processed from a related precursor nucleobindin 1 (NUCB1). Here we determined if NLP, like NESF-1, regulates lipid accumulation in vitro, and tested if the disruption of *nucb1* gene affects hepatic lipid metabolism genes in mice. Hepatocytes (HepG2/C3A cells) express NLP and NESF-1 and both peptides significantly reduced lipogenic enzyme mRNAs and enhanced beta-oxidation enzyme mRNAs. Lipid contents in oleic acid induced HepG2/C3A cells were attenuated by NESF-1 and NLP. The inhibitory effect on cellular lipid content was blocked by compound C, an inhibitor of AMPK. The disruption of *nucb1* gene affected lipid metabolism-related enzyme mRNAs, endogenous *nucb2* mRNA and AMPK phosphorylation. The lipid-lowering effects identified here highlights the potential of nucleobindins and peptides processed from them to address lipid disorders, and its possible benefits in metabolic disease management.

Nucleobindin 1 (NUCB1) is a calcium- and DNA-binding, 55 kD multi-domain protein. This protein was reported in cellular Golgi apparatus¹ and nucleus² and was found to be secreted from cells³. NUCB1 is highly conserved in mammals and non-mammals⁴. Another member of nucleobindin family was named NUCB2 due to high similarity to NUCB1. Nesfatin-1 (NESF-1) (NEFA/nucleobindin 2 encoded satiety and fat influencing protein), an 82 amino acid peptide processed from the N-terminal region of NUCB2 was reported in 2006⁵. This peptide has received considerable attention due to scientific findings implicating its role in the regulation of food⁵ and water⁶ intake, lipid⁷ and glucose⁸ metabolism, insulinotropic effect⁹, reproduction¹⁰, and sleep¹¹. NUCB2 is expressed in hypothalamus^{5,12}, pituitary¹², pancreas^{8,13}, gastrointestinal tract^{13,14}, and testis¹³. The presence of NUCB2 (precursor) and NESF-1 (processed peptide) in central and peripheral endocrine tissues suggests pleiotropic effects. NESF-1 has also been implicated in the regulation of lipid metabolism in different tissues, including white adipose tissue (WAT) and liver.

Chronic central infusion of NESF-1 reduced bodyweight gain, and subcutaneous and visceral fat mass of Wistar rats⁵. NESF-1 reduced lipid accumulation in 3T3-L1 mouse preadipocytes and inhibited the expression

peroxisome proliferator-activated receptor (*Ppar*) γ , fatty acid binding protein (*Fabp*) 4 and *Cfd* (adipsin) mRNAs in differentiated adipocytes¹⁵. On the other hand, a clear inhibition of cell proliferation and an increase in adipocyte differentiation were reported in *Nucb2* knockdown group of 3T3-L1 preadipocytes¹⁶. Moreover, peripheral infusion of NESF-1 attenuated lipid accumulation in hepatocytes through AMP-activated protein kinase (AMPK)-mediated pathway in diet-induced obese mice⁷. A significant reduction in serum NESF-1 in patients with non-alcoholic fatty liver (NAFLD) disease was reported¹⁷. These observations indicate a potential role for NESF-1 in the regulation of lipid metabolism.

Very recently, it has been proposed that NUCB1 has a NESF-1-like peptide (NLP) sequence, which is putatively processed by prohormone convertases (PCSKs). *Nucb1* and *Nucb2* shared 60% sequence homology in the mouse genome¹⁸. It was reported that the bioactive core of murine NLP and NESF-1 shares 76% amino acid sequence homology¹⁹. The presence of NLP in similar anatomical locations as NESF-1, including the pancreas, pituitary, gonads, and gut was reported^{19,20}. Similarly, NLP was shown to suppress food intake and modulate the expression of appetite-regulatory hormones

¹Laboratory of Integrative Neuroendocrinology, Department of Veterinary Biomedical Sciences, Western College of Veterinary Medicine, University of Saskatchewan, Saskatoon S7N 5B4 Saskatchewan, Canada. ²Department of Anatomy, Physiology and Pharmacology, College of Medicine, University of Saskatchewan, Saskatoon S7N 5E5 Saskatchewan, Canada. e-mail: suraj.unniappan@usask.ca

in goldfish²⁰ and rats. Based on the similarities on its sequence, tissue distribution, and biological actions of NLP and NESF-1, we hypothesized that NLP too elicit NESF-1 effects in decreasing lipid accumulation in hepatocytes. We tested this hypothesis using human hepatocytes (HepG2/C3A cells) and genetically modified mice.

Results

HepG2/C3A cells express NUCB1 and NUCB2

To determine whether hepatocytes express NUCBs, localization of NUCB1 and NUCB2 in HepG2/C3A cells was carried out using immunocytochemistry (ICC) based on our previously reported protocols²¹. HepG2/C3A cells are immunoreactive for NUCB1/NLP (green, Fig. 1a) and NUCB2/NESF-1 (green, Fig. 1b). DAPI stained cell DNA in blue color. NUCB1/NLP-like immunoreactivity was mainly observed in the nucleolus. In contrast, NUCB2/NESF-1 like immunoreactivity was mainly observed in the cytoplasm of cells and was also detected in the nucleus of some cells. No immunoreactivity was observed for the negative control group, which was incubated with only the secondary antibody (Supplementary Fig. 1).

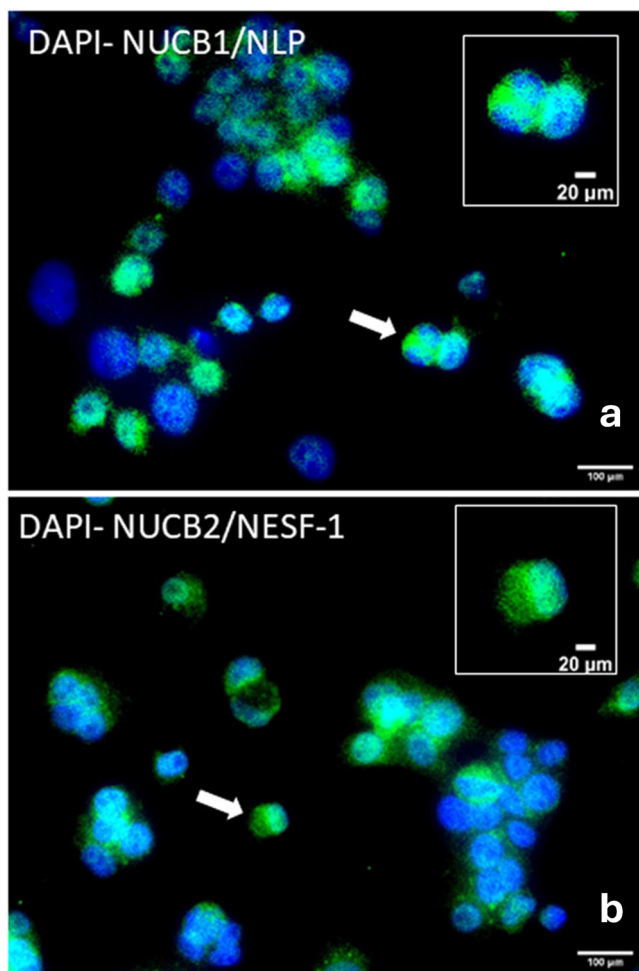


Fig. 1 | HepG2/C3A cells express NUCB1/NLP and NUCB2/NESF-1. HepG2/C3A cells express NUCB1/NLP (a) and NUCB2/NESF-1 (b) in green color. DAPI stained DNA in blue color. The arrows point to magnified hepatocytes shown in insets. Scale bar = 100 μ m, or 20 μ m (inset images). DAPI stained DNA in blue color. Primary antibodies used are: rabbit anti-mouse NUCB1 (1:250, custom synthesized, cat no. 1312-PAC-02, Pacific Immunology, USA), rabbit anti-mouse NUCB2 (1:250, RRID: AB_2891124, cat no. 1312-PAC-01, Pacific Immunology, USA). Secondary antibodies used are: goat anti-rabbit Alexa Fluor[®] 488 (1:500, RRID: AB_2630356, cat no. ab150077, ABCAM, UK).

NLP and NESF-1 affected the expression of enzymes involved in hepatic lipid synthesis in untreated and oleic acid (OA)-induced HepG2/C3A cells

The possible regulatory effects of NLP and NESF-1 on the abundance of mRNAs for enzymes involved in hepatic lipid synthesis and beta-oxidation were studied. As shown in Fig. 2a–d, NLP, and NESF-1 at 0.1 nM decreased lipogenic acetyl-CoA carboxylase (*ACC*), glycerol-3-phosphate acyltransferase (*GPAM*), sterol regulatory-element binding factor (*SREBF-1*) and carnitine palmitoyl transferase (*CPT-1 α*) and increased 3-hydroxy-3-methylglutaryl-coA reductase (*HMGCR*) in untreated HepG2/C3A cells at 24 h post incubation. NLP also decreased the expression of fatty acid synthase (*FASN*), diacyl glycerol acyltransferase (*DGAT*) 1, *DGAT*2 and long-chain acyl coA dehydrogenase (*ACADL*) at the same time point.

Specifically, NLP and NESF-1 at 0.1 nM decreased lipogenic *ACC*, *GPAM*, and *SREBF-1*, but increased *HMGCR* mRNA at 24 h post incubation (Fig. 2a, b). Both peptides decreased *CPT-1 α* mRNA expression in the same experiment (Fig. 2c, d). Moreover, NLP decreased the expression of *FASN*, *DGAT*1, *DGAT*2, and *ACADL* mRNA in HepG2/C3A cells at 24 h post incubation (Fig. 2a, c).

NLP and NESF-1 at 0.1 nM decreased the expression of lipogenic *ACC*, *GPAM*, *SREBF-1*, and *HMGCR*, while increasing *CPT-1 α* (beta-oxidation) at 24 h post incubation (Fig. 3a–d). Positive control, quercetin, at 10 μ M decreased the expression of lipogenic *ACC*, *SREBF-1* and *HMGCR* but did not show any effect on *GPAM*. Similar to NESF-1 and NLP, quercetin increased the *CPT-1 α* mRNA level at 24 h post incubation.

NLP and NESF-1 decreased Oil Red O (ORO) staining area in OA-induced HepG2/C3A cells

In order to determine whether lipid accumulation in HepG2 cells (Fig. 4a) is modulated by nesfatin-1 or NLP, we treated HepG2/C3A cells with oleic acid (Fig. 4b) and stained the cells with the lipid stain Oil Red O. NLP (Fig. 4d) and NESF-1 (Fig. 4c) decreased the ORO lipid staining area by approximately 11% when compared to OA control group (Fig. 4b) as assessed by lipid staining area (Fig. 4f) of 5–7 images per group using ImageJ software. Quercetin (positive control; Fig. 4e) also caused a similar decrease in the lipid staining area in OA-induced HepG2/C3A cells (Fig. 4f). The effect of quercetin was not statistically different from the effects of NESF-1 and NLP.

AMPK has been suggested as an involving intracellular signaling molecule for treating several chronic diseases, such as type 2 diabetes and obesity. AMPK is a serine/threonine protein kinase that possesses a fundamental role in the regulation of cellular energy homeostasis in mammalian cells. This molecule is activated upon depletion of cellular energy²². Then, activated AMPK induces ATP generation pathways such as glycolysis, fatty acid oxidation and lipolysis while inhibiting anabolic pathways, including lipid and protein synthesis. Polyphenolic compounds, for example, quercetin were shown to attenuate lipid accumulation in HepG2/C3A cells through the AMPK-mediated pathway²³. Moreover, NESF-1 was reported to increase phosphorylated (P)-AMPK α /Total(T)-AMPK α in the primary culture of mouse hepatocytes⁷. Since NLP and NESF-1 share identical amino acid sequences, especially within the putative bioactive core across vertebrates, we hypothesized that NLP and NESF-1 might act through AMPK pathway to regulate hepatic lipid synthesis and oxidation. To determine the cell signaling mediators, HepG2/C3A cells were incubated with fresh media (control group) or NLP/NESF-1/quercetin (experimental groups) at effective doses for 2 h, and then P-AMPK α /T-AMPK α ratio was assessed in cell lysate. As shown in Fig. 5a, 0.1 nM of NLP and NESF-1 significantly increased P-AMPK α /T-AMPK α ratio at 2 h post incubation. Quercetin exerted the same effects on P-AMPK α /T-AMPK α ratio. The inhibition of AMPK by compound C resulted in a significant increment of triglyceride (TG) content in OA-induced HepG2/C3A cells (Fig. 5b). Furthermore, NLP and NESF-1 attenuated the cellular TG, which was 1.8-fold less than the OA control. Quercetin exerted similar effects on cellular TG. The cellular TG levels in OA control was 3.6-fold higher than what was found in untreated HepG2/C3A cells.

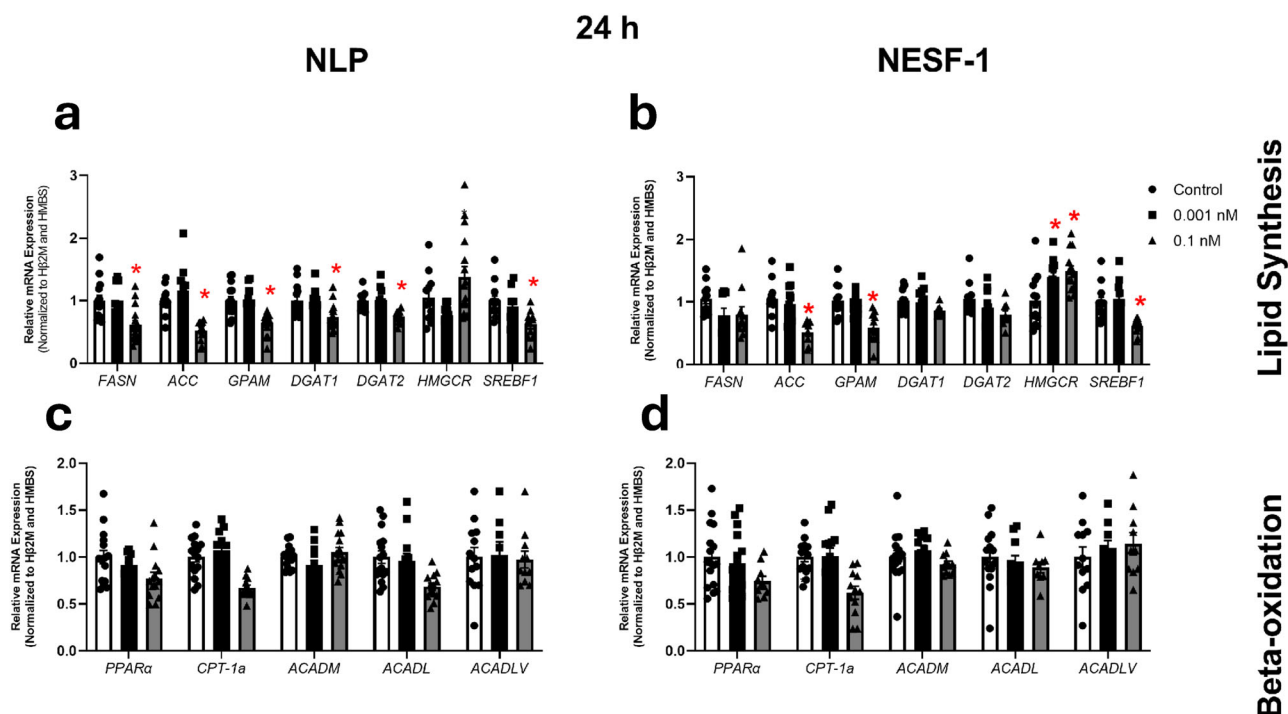


Fig. 2 | NESF-1 and NLP modulate hepatic lipogenic and beta-oxidation enzyme mRNAs. NLP and NESF-1 (0.001 or 0.1 nM) affected the expression of hepatic lipogenic (a, b) and beta-oxidation (c, d) enzyme mRNAs in HepG2/C3A cells at 24 h post incubation. All data are represented as mean ± SEM. Results presented are pooled from three independent studies with at least triplicates for each treatment within each study. Asterisks indicate significant differences between experimental group (each concentration) and corresponding control (untreated

cells) for mRNA quantified. Significance was set at $P < 0.05$. mRNAs measured are: acetyl-CoA carboxylase (*ACC*), glycerol-3-phosphate acyltransferase (*GPAM*), sterol regulatory-element binding factor (*SREBF*)-1, carnitine palmitoyl transferase (*CPT*)-1 α , 3-hydroxy-3-methylglutaryl-coA reductase (*HMGCR*), fatty acid synthase (*FASN*), diacyl glycerol acyltransferase (*DGAT*) 1, *DGAT*2 and long/very long-chain acyl coA dehydrogenase (*ACADL*; *ACADLV*), peroxisome proliferator-activated receptor (*Ppar*) γ , acyl CoA dehydrogenase medium chain (*ACADM*).

NLP and NESF-1 affected *NUCB* mRNAs and *NUCB* proteins in OA-induced HepG2/C3A cells

The addition of nesfatin-1 or NLP could influence the abundance of endogenous forms of these peptides produced within HepG2 cells and this was tested. NESF-1 upregulated *NUCB1* mRNA while downregulated *NUCB2* mRNA. In contrast, NLP had no effects on *NUCB1* mRNA, but upregulated *NUCB2* mRNA in OA-induced cells. The endogenous level of *NUCB2* mRNA was decreased in OA-induced cells compared to untreated cells (Fig. 6a). Similarly, NESF-1 enhanced *NUCB1* protein level while decreasing *NUCB2* protein. Moreover, NLP enhanced *NUCB2* protein level in OA-induced HepG2/C3A cells (Fig. 6b).

The genetic disruption of *Nucb1* gene affected lipid pathways-related enzymes and *Nucb* mRNAs in mice liver in a sex- and diet-specific manner

The genetic disruption of *Nucb1* downregulated the expression of lipogenic genes (*Acc*, *Fasn*, *Gpam*, *Hmgcr*, *Srebf*-1) in female mice fed 60% high-fat diet (Fig. 7a) and showed a similar pattern in male mice (Fig. 7b), causing a decrease in *Acc*, *Fasn*, and *Srebf*-1 mRNA abundance. Although the disruption in *Nucb1* gene did not affect beta-oxidation-related genes in female mice (Fig. 7c), it upregulated the expression of some of these genes (*Cpt*-1 α , *Acadl*, *Acadlv*, and *Acadm*) in male mice (Fig. 7d). The difference in the expression of lipogenic and beta-oxidation genes shows a sex-specific effect of *Nucb1* and *Nucb2* gene disruption. Meanwhile, the expression of neither lipogenic genes nor beta-oxidation genes were affected by the disruption of *Nucb1* or *Nucb2* in male or female mice fed 10% fat diet (Fig. 7f–i). The only exception to this was a reduction in *Fasn* in male *Nucb1*-disrupted mice (Fig. 7g). The genetic disruption in *Nucb1* resulted in the upregulation of *Nucb2* mRNA in male mice fed 60% fat diet (Fig. 7e), but not in female mice (Fig. 7e). However, such a change in *Nucb2* mRNA was not observed in the same strains of male or female mice fed 10% fat diet (Fig. 7j).

Three-way ANOVA analysis showed that the main effect of “diet” and “gene disruption” on lipogenic enzyme transcripts in *Nucb1*-disrupted mice was significant. In this regard, the two-way interaction of “diet × gene disruption” on these transcripts in both groups was also statistically significant. Furthermore, the significant effect of two-way interactions “diet × sex” and “sex × gene disruption” were observed for some lipogenic genes expression in *Nucb1* gene-disrupted mice. Three-way ANOVA analysis demonstrated that the main effect of “diet” and “gene disruption” on beta-oxidation-related gene expression were significant in the *Nucb1*-disrupted group. The interaction of “diet × gene disruption” for *Nucb1* group was statistically significant.

The genetic disruption of *Nucb1* increased the ratio of P-AMPK α /T-AMPK α in mice liver in a sex-specific manner

The genetic disruption of *Nucb1* increased the ratio of hepatic P-AMPK α /T-AMPK α in the male mice fed high-fat diet (Fig. 8a), while there were no significant changes in AMPK ratio in female mice (Fig. 8b). This shows the sex-specific effect for the genetic disruption in *Nucb* genes on lipid synthesis and beta-oxidation-mediated pathways.

Discussion

In this research, first we assessed whether *NUCB1*/NLP and *NUCB2*/NESF-1 are present in human hepatocytes, explored if they act directly to regulate lipid accumulation in untreated and OA-induced HepG2 cells, and elucidated some cellular pathways mediating such effects. *NUCB1*/NLP-like immunoreactivity was reported in the central nervous system and peripheral tissues, including endocrine cells of the anterior pituitary of rats and mice^{21,24}, mouse insulinoma MIN6 cell line and mouse pancreatic beta cells¹⁹ as well as the testis, ovary and pituitary of goldfish²⁰. The immunoreactivity of *NUCB1*/NLP was primarily found in cell cytoplasm in mammalian central and peripheral tissues^{21,24,25}. In contrast, *NUCB1*/NLP was mainly detected in nucleus and in some cells in the cytoplasm, which suggests a cell- and

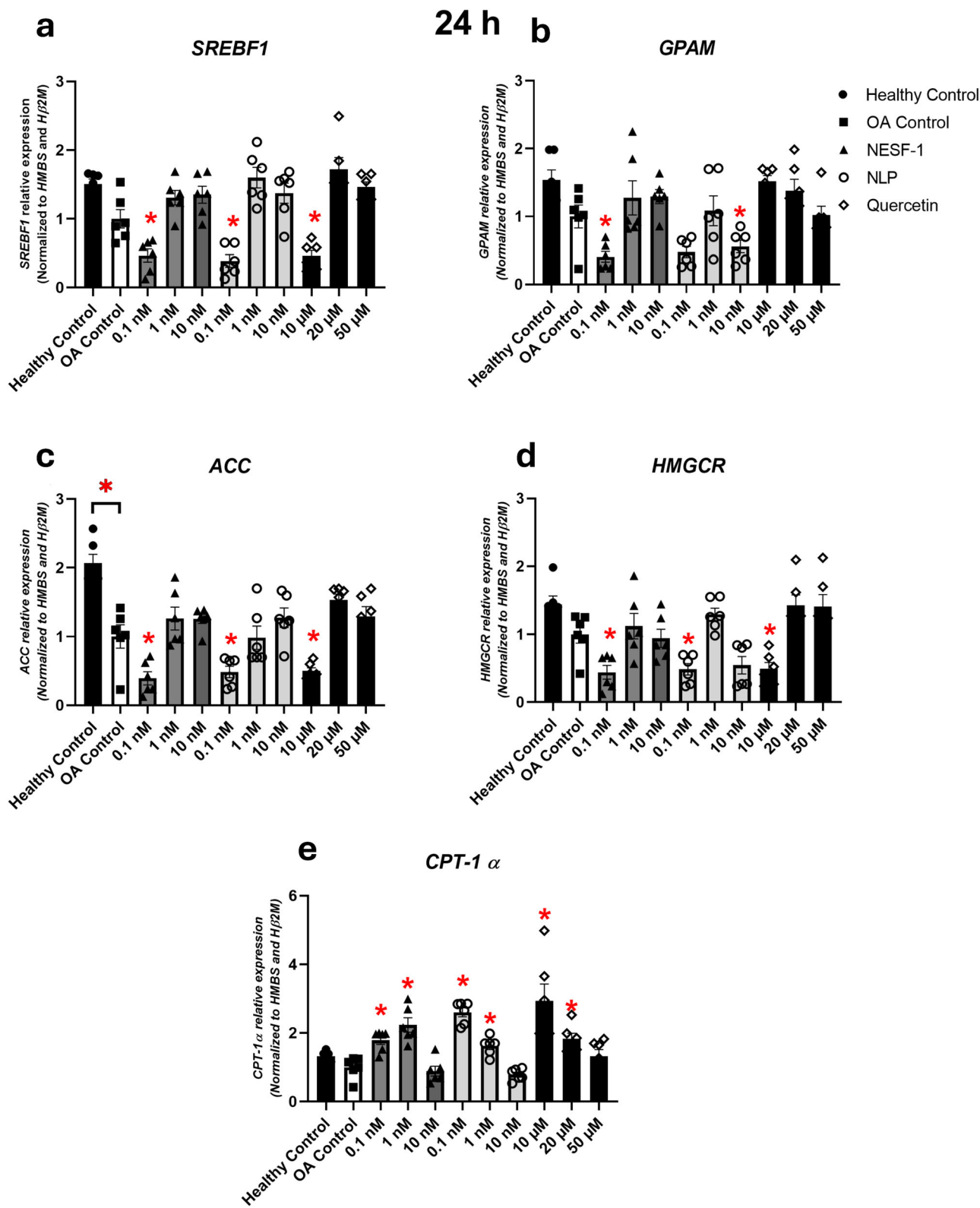
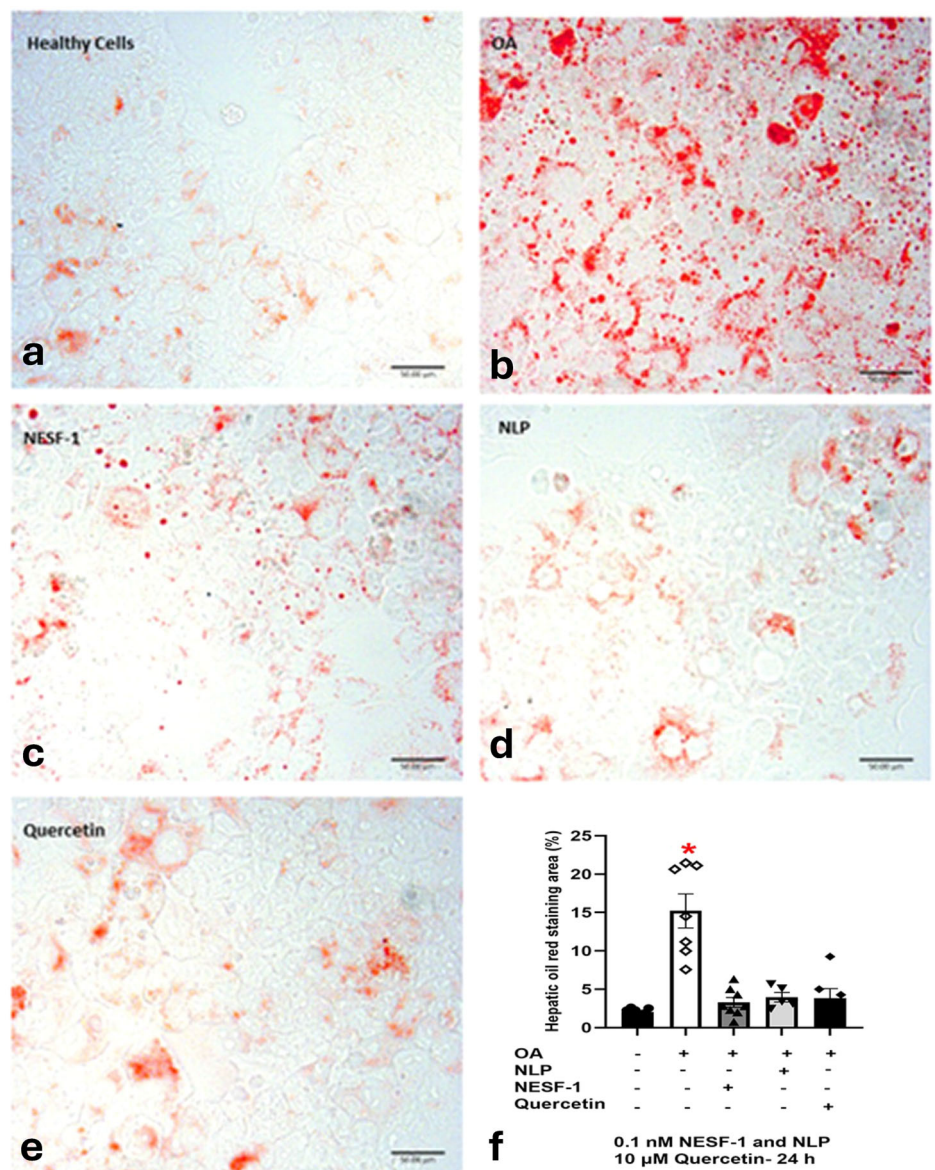


Fig. 3 | NESF-1 and NLP affected lipid metabolism enzyme mRNAs in oleic acid-treated cells. NLP and NESF-1 (0.1–10 nM) and quercetin (10 μ M) affected the expression of hepatic lipogenic (a–d) and beta-oxidation (e) enzymes at mRNA level in OA-induced HepG2/C3A cells at 24 h post incubation. All groups were pretreated with OA except untreated controls. All data are represented as mean \pm SEM. Results

presented are pooled from three independent studies with at least triplicates for each treatment. Asterisks show the significant difference between the experimental group (each concentration) and the corresponding OA control for each gene. Significance was set at $P < 0.05$.

Fig. 4 | Nesfatin-1 and NLP reduced lipid content staining in oleic acid-treated cells. These pictures show Oil Red O (ORO) staining in HepG2/C3A cells (a). Scale bar = 50 μ m. All groups were pretreated with oleic acid (OA; b) except untreated controls. NLP (d; 0.1 nM) and NESF-1 (c; 0.1 nM), and quercetin (e; 10 μ M) decreased ORO lipid staining area in OA-induced HepG2/C3A cells at 24 h post incubation. HepG2/C3A cells were fixed with 4% paraformaldehyde and then stained with ORO. The ORO staining area (f) within cells was measured by ImageJ software (5–7 images/group). All data are represented as mean \pm SEM. Asterisks show the statistically significant difference between each group and untreated controls. Significance was set at $P < 0.05$.

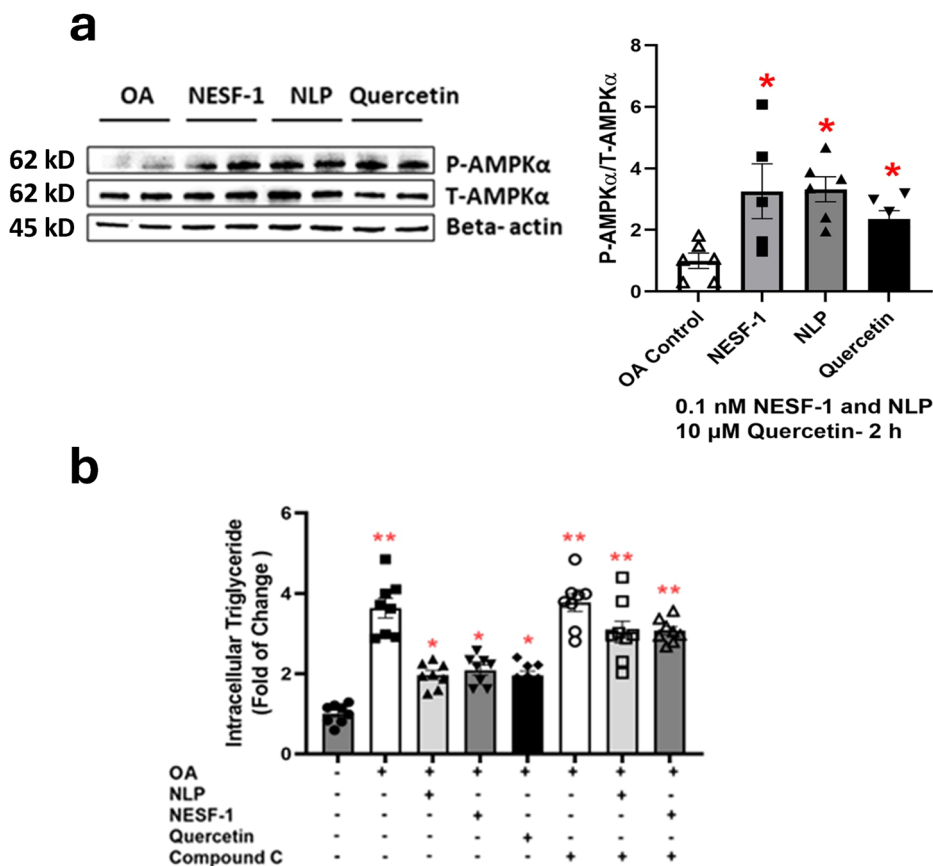


tissue-specific pattern of NUCB1/NLP distribution. Similar to NUCB1/NLP, NUCB2/NESF-1 immunoreactivity was observed in both central and peripheral tissues and cells, including rat anterior pituitary and hypothalamic nuclei^{24,26}, mouse corticotrophs²¹, human hypothalamus, rodent duodenum, esophagus, liver, intestine and colon¹⁴. Different in vitro and in vivo studies reported the positive immunoreactivity of NUCB2/NESF-1 in the cytoplasm of neurons originated from rat and mouse brain^{21,24,27}, and in the nuclei of endothelial cells of mouse lung²⁸. NUCB2/NESF-1-like immunoreactivity was observed in cytoplasmic vesicles of cells in peripheral tissues, including gastric cells³⁹ and rat Leydig cells³⁰. NUCB1 and nesfatin-1 immunoreactivity was reported in embryonic and adult mouse liver, suggesting a local role for these peptides³¹. NUCB1 and NUCB2 mRNA and their proteins were upregulated in NESF-1- and NLP-treated HepG2/C3A cells, respectively. We previously reported that the addition of NLP and NESF-1 suppressed endogenous *Nucb* mRNAs in mouse corticotrophs²¹. It is suggestive of a potential negative feedback loop that causes a reduction in endogenous *Nucb* production when exogenous NESF-1 or NLP are present. These discrepancies in *Nucb* expression upon nesfatin-1 or NLP treatment reported here and in our previous research suggest species- and cell-specific pattern for the changes in endogenous NUCB production. Together, these results suggest that human hepatocytes

are possibly a cell source of endogenous NUCB and processed peptides. The presence of a signal peptide and processing enzymes suggest secretion of NUCBs and processed peptides from hepatocytes. The hepatic secretory profile of these peptides and whether the endogenous peptides might play a role in hepatic lipid synthesis in hepatocytes warrant further consideration.

Previous studies reported the effect of NESF-1 on glucose and lipid metabolism in rodents and in vitro in goldfish primary hepatocytes, suggesting the presence of a functional receptor for this peptide in the liver^{7,32}. We further examined how NLP and NESF-1 regulate the expression of enzymes involved in lipid synthesis and lipid oxidation in human HepG2/C3A cells. A clear downregulation of some lipogenic and beta-oxidation genes in untreated HepG2/C3A cells was observed at 24 h post incubation with 0.1 nM NESF-1 or NLP. In the next step, how these two peptides and quercetin affect lipid accumulation in OA-induced HepG2/C3A cells was determined. Interestingly, both peptides at 0.1 nM and quercetin at 10 μ M downregulated lipogenic enzyme expression and upregulated the beta-oxidation gene expression at 24 h post incubation. Continuous peripheral administration of NESF-1 significantly downregulated lipogenic genes and transcription factors in liver samples of male C57BL/6J mice fed 60% fat diet, which agrees with our findings on the regulatory effect of NESF-1 on enzyme expression involved in lipid synthesis⁷. Adipose tissue ppar a, fasn,

Fig. 5 | Nesfatin-1 and NLP increased AMPK phosphorylation in oleic acid-treated cells. NLP and NESF-1 (0.1 nM) and quercetin (10 μM) increased the phosphorylation of AMPK in OA-induced HepG2/C3A cells after 2 h post incubation (a). Primary antibodies: polyclonal rabbit anti-phospho (Thr172)-AMPKα antibody (1:1000, RRID: AB_330330, cat no. 2531 S, Cell Signalling, USA), polyclonal rabbit anti-AMPKα antibody (1:1000, RRID: AB_330331, cat no. 2532 S, Cell Signalling, USA). The secondary antibodies: goat anti-rabbit IgG (H + L)-HRP conjugate antibody (1:5000, RRID: AB_11125142, cat no. 170-6515, Bio-Rad, USA) and goat anti-mouse IgG (H + L)-HRP conjugate antibody (1: 5000, RRID: AB_11125547, cat no. 170-6516, Bio-Rad, USA). Studying the NLP and NESF-1 mechanism of action on HepG2 to decrease lipid accumulation in HepG2 cells (b), HepG2 cells were treated with compound c (10 μM) for 1 h and then NLP/NESF-1/Quercetin were added to media for 24 h. Results for both parts presented are pooled from three independent studies with duplicate for each treatment. All groups were pretreated with OA except untreated controls (a, b). All data are presented as mean ± SEM. Asterisk shows the significant difference between each group and OA control (a, b) while two asterisks show the significant difference between each group and untreated controls (b). Significance was set at $P < 0.05$.



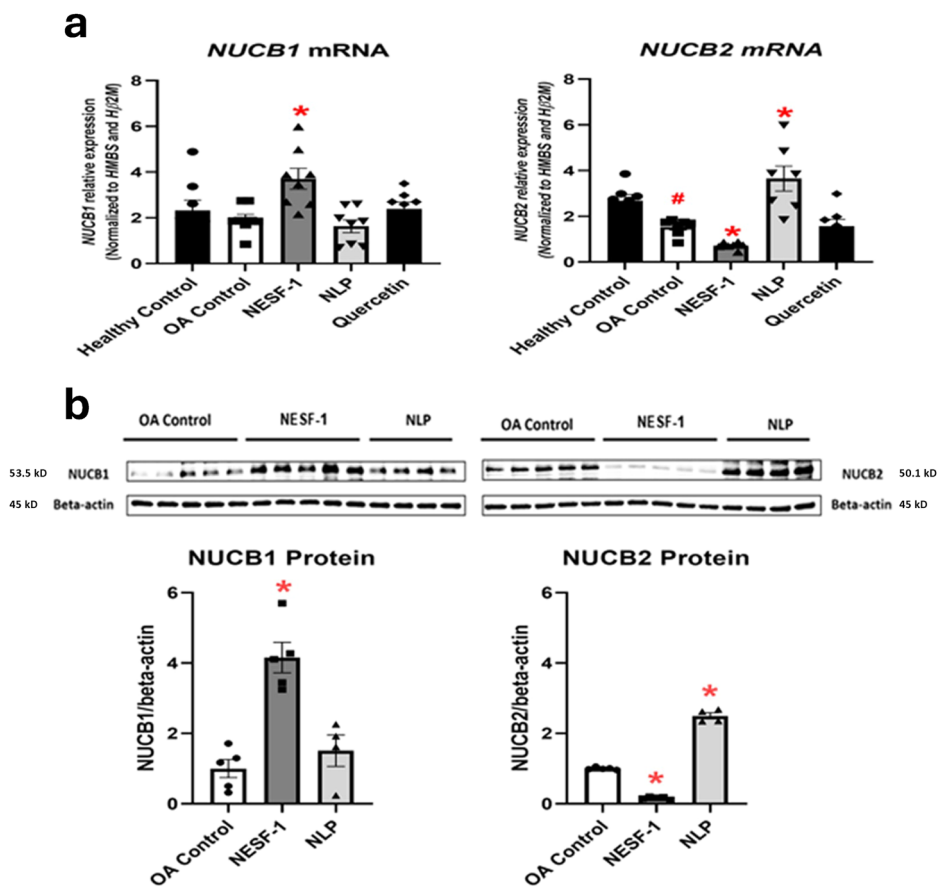
ppam and slc27a1 were significantly reduced in the white adipose tissue of C57BL/6 J mice continuously infused with 2.5 pmol/mouse/hour nesfatin-1 for 2 weeks. Similarly, the abundance of ppar a, srebp 1, acaca, fasn, gpam, dgat1, and dgat 2 were significantly reduced in the liver of nesfatin-1 infused high-fat diet-fed C57BL/6 mice, but not in mice fed regular chow. In addition, Yin and colleagues⁷ conducted in vitro studies very similar to ours, but using primary hepatocyte derived from C57BL/6J mice. In alignment with the results presented here, primary hepatocyte expression of lipogenic genes srebf-1, srebf2, acaca, fasn, gpam, and dgat1 were suppressed by nesfatin-1. Meanwhile, lipid oxidation genes ppar a, cpt-1 a, acadm, acadl, acadvl and atgl were significantly upregulated by nesfatin-1. While our results reproduced these results in human hepatocytes, it also provided evidence for comparable effects for NLP on effects. NESF-1 was also reported to decrease the expression of lipogenic genes, *Acc* and *Fasn*, in primary brown adipocytes of mice³³. Moreover, NESF-1 treatment significantly decreased *srebf-1* and enhanced *lpl* and *cpt-1α*, which decreased lipogenesis capacity and increased beta-oxidation in the liver of rainbow trout³⁴. Therefore, the comparable biological effects of NESF-1 and NLP are likely due to the high degree of amino acid sequence similarity. Quercetin, the positive control used in our research was widely reported to alleviate lipid accumulation in vitro and in vivo by affecting mRNAs and proteins encoding enzymes within the lipid metabolic pathways. A dose-response was observed for quercetin at a range of 0.1–100 μM, which was associated with *SREBF-1* and *FASN* downregulation in vitro lipid accumulation model using HepG2 cells³⁵. In our study, the suppressive effect of quercetin on lipogenic genes was observed within the dose range reported in the study mentioned above.

To estimate lipid accumulation, we then stained lipid droplets using ORO dye. ORO specifically stains the TG and cholesteryl oleate, but not other lipids³⁶. Since the hallmark of NAFLD is the TG accumulation in the cytoplasm of hepatocytes³⁷, ORO staining can histologically evaluate changes in lipid accumulation. Our results showed that cellular TG was

almost undetectable in untreated HepG2/C3A cells. The average stained lipid area decreased remarkably in the NLP and NESF-1 treated group relative to the OA-induced control group. To confirm our ORO staining-based results, cellular TG in HepG2/C3A cells treated with NLP, NESF-1 and quercetin was then measured. Consistently, both NLP and NESF-1, along with the positive control, decreased TG accumulation by approximately twofold in OA-induced HepG2/C3A cells. Similar to our results, peripheral infusion of NESF-1 decreased both ORO-based average area and diameter of lipid droplets in the liver as well as plasma and hepatic TG content in diet-induced obese mice⁷. Furthermore, quercetin was shown to affect lipid accumulation in a dose-dependent manner (1–100 μM) evaluated by an ORO-based colorimetric quantitative assay. The onset of the lipid-lowering effect of quercetin started at 10 μM in the previous study³⁵ and this is in agreement with the findings reported here. Plasma nesfatin-1 levels were significantly elevated in a rat model of NAFLD³⁸. Meanwhile, serum nesfatin-1 levels were found reduced in patients with NAFLD¹⁷. While species-specific changes in NAFLD nesfatin-1 profile exists, it is evident that one of the proteins changed in NAFLD is nesfatin-1. Whether NUCB1 and NLP also shows a similar NAFLD profiles is unknown. The role of endogenous NUCBs and processed peptides and its possible role in liver lipid metabolism and NAFLD is also currently unclear.

To assess the potential signaling pathway mediating the lipid attenuation effect of NLP, NESF-1, and quercetin, we first checked the phosphorylation of AMPK at different time points. Although studies on NLP and NESF-1 and its biological roles in different species have progressed well, identifying different cellular cascades mediated by NLP and NESF-1, and their receptor are poorly understood. Labeled-NESF-1 and NLP bind to the surface of rat GH3 cells, suggesting that the effects of these two peptides are mediated by a G-protein coupled receptor (GPCR)²⁴. It was reported that NESF-1 stimulates the cellular intake of calcium in the rat hypothalamus neuronal cell culture due to its binding to GPCRs. This effect was blocked when a GPCR disruptor was added to the media³⁹. Another study

Fig. 6 | Nesfatin-1 and NLP influenced *NUCB* mRNAs and *NUCB* protein in oleic acid-treated cells. NLP and NESF-1 (0.1 nM) affected *NUCB* mRNA (a) and *NUCB* protein (b) in OA-induced HepG2/C3A cells at 24 h post incubation. All groups were pretreated with oleic acid (OA) except untreated control. Results presented for *NUCB* mRNA (a) are pooled from three independent studies with at least triplicates for each treatment. Results presented for *NUCB* protein (b) were pooled from two independent studies with duplicates or triplicates for each treatment ($n = 4-5$ samples in total/group). All data are represented as mean \pm SEM. Asterisks show the difference between the experimental group and the OA control. Significance was set at $P < 0.05$.



proposed GPCR12 as a potential receptor for NESF-1⁴⁰. Our results suggest the possible presence of a functional NESF-1/NLP receptor in hepatocytes. The activation of this receptor may lead to the phosphorylation AMPK and, subsequently, the alternation in the expression of enzymes involved in lipogenesis. Previous studies confirmed that intervention with AMPK activity by pharmacological approaches is linked with lipid metabolism in the liver⁴¹. Consistent with pharmacological studies, genetic deletion of AMPK β 1 enhanced lipogenesis while decreasing beta-oxidation in primary culture of hepatocytes. Moreover, AMPK α 2 is essential for the hypolipidemic and antisteatotic effects of n-3 long-chain polyunsaturated fatty acids effects in mice⁴². Our results also showed that the inhibition of AMPK by compound C resulted in the accumulation of TG in HepG2/C3A cells. NLP, NESF-1, and quercetin failed to decrease lipid accumulation in the presence of compound C in OA-induced HepG2/C3A cells. Consistently, NESF-1, NLP and quercetin activated AMPK in HepG2/C3A cells. In line with our result, NESF-1 failed to decrease TG accumulation in cultured mouse hepatocytes in the presence of compound C, an AMPK inhibitor⁷. Meanwhile, AICAR, a selective activator of AMPK reduced triglyceride contents in liver cells. Another study revealed that infusion of NESF-1 into the third cerebral ventricle of high-fat diet-fed rats increased hepatic insulin sensitivity through the AMPK-mediated pathway⁴³. Moreover, central NESF-1 activated fatty acid oxidation in the muscle through the AMPK-mediated pathway in mice with streptozotocin-induced type 2 diabetes mellitus⁴⁴. Consistent with our results, in vitro and in vivo studies showed that quercetin improves lipid and glucose metabolism through the AMPK-mediated pathway^{23,45,46}. Altogether, an unknown GPCR for nesfatin-1/NLP acting through an AMPK-mediated pathway appears to mediate NLP and NESF-1 effects on lipid accumulation in human HepG2/C3A cells.

In the next step, we assessed whether the disruption of *Nucb1* gene affects the expression of enzymes involved in lipid synthesis and oxidation.

We also examined the effect of sex, *Nucb1* absence and diet on the expression of genes involved in lipid synthesis. Previous studies reported that feeding a high-fat/high fructose diet resulted in marked sex- and strain-specific changes in the expression of genes involved in lipid synthesis in the liver of male and female mice, with all four hepatic lipid metabolic pathways altered⁴⁷. Another study reported sexual dimorphism of hepatic cholesterol metabolism in exposure to dietary cholesterol in high-fat-fed mice⁴⁸. The results of the current study show that feeding a high-fat diet resulted in changes in gene expression patterns across all mouse groups; however, the severity of these effects was dependent on either sex, *Nucb1* gene disruption or the compensatory upregulation of the other *Nucb*. However, lipogenic and beta-oxidation gene pattern in in vitro studies showed a similar pattern where both *NUCB* genes exist in HepG2/C3A cells. These results show that other regulatory signals beyond liver may control lipid metabolism, such as plasma lipid profile, neuroendocrine signals, lipid metabolism state in adipose tissue and muscles. A direct comparison of the in vivo study results to that from the in vitro studies is more complicated due to two reasons. First, the endocrine and metabolic milieu in these mice is multifactorial. Thus, the direct actions of nesfatin-1/NLP shown in human hepatocytes is not comparable to the mouse studies. Species-specific differences also exist, and the example of circulating nesfatin-1 levels in NAFLD in humans and rats discussed earlier is one example for that. In addition, the global changes that occurs due to embryonic disruption of one gene might alter this milieu as well as compensatory changes in other lipid regulators. Therefore, the changes noted in the knockout mice are multifactorial, not solely due to the disrupted gene. Furthermore, the genetic disruption in *Nucb1* upregulated *Nucb2* in a sex-specific manner. This suggests a compensatory response in the upregulation of one *Nucb* during the genetic interruption of the other *Nucb*. Consistently, upregulation of AMPK phosphorylation was observed in *Nucb1* gene disrupted male mice but not in female mice which might be due to the upregulation of

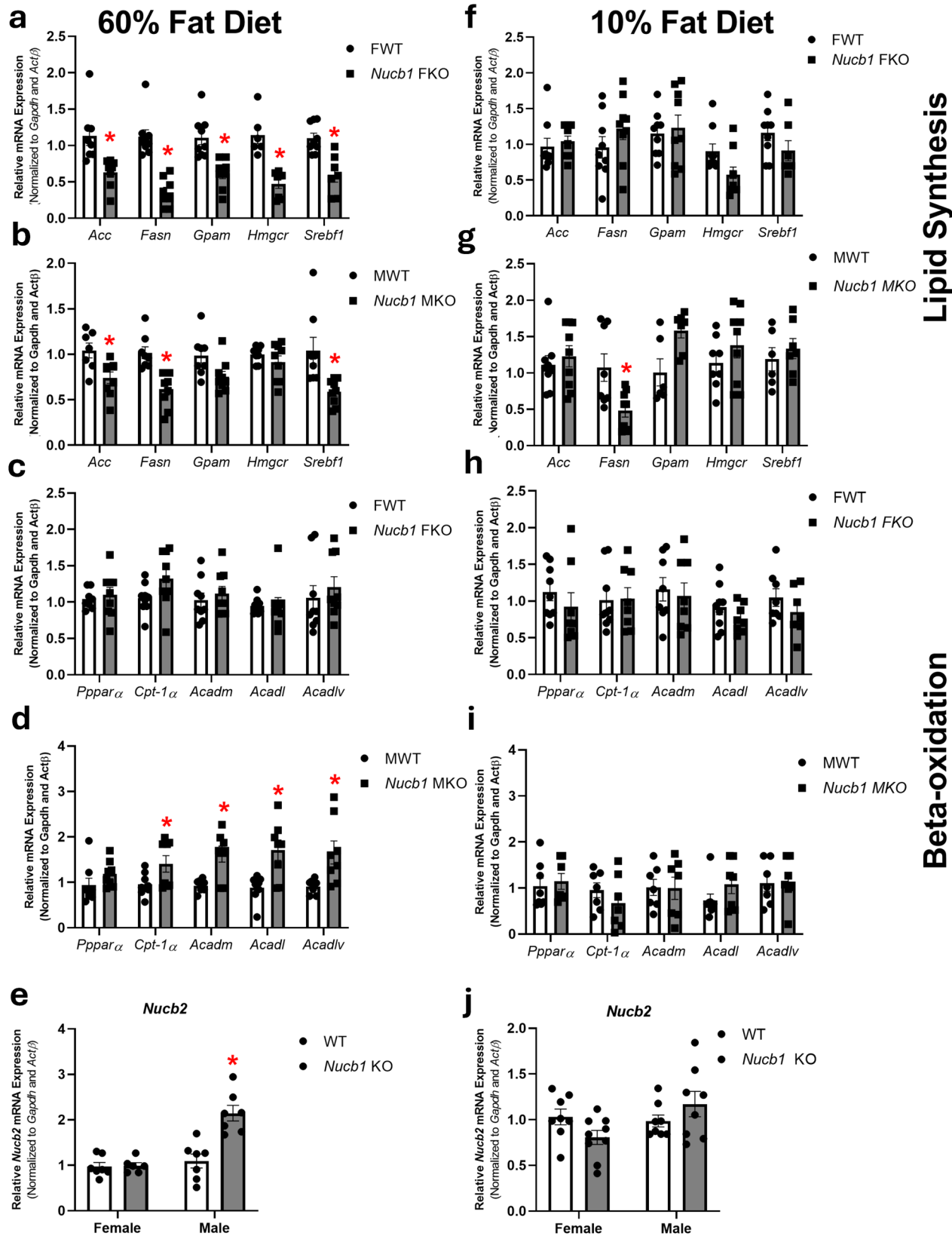


Fig. 7 | *NUCB1* disruption caused changes in lipid metabolism-regulating enzyme mRNAs. The genetic disruption of *Nucb1* affected lipid pathways-related enzymes (a–d = 60% fat diet-fed; f–i = 10% fat diet-fed) and *Nucb* mRNAs (e = 60% fat diet-fed; j = 10% fat diet-fed) in the liver of mice fed 60% fat diet (left panel), or 10% fat diet (right panel) in a sex- and diet-specific manner. All data are represented as mean ± SEM. The results presented are pooled from at least 7 liver samples (from individual mouse) per group. Asterisks show significant differences between knockout (male/M *Nucb1* or

female/F *Nucb1*; gray bar) and wild-type (WT; white bar) groups. Significance was set at $P < 0.05$. mRNAs measured are: Acetyl-CoA carboxylase (*ACC*), glycerol-3-phosphate acyltransferase (*GPAM*), sterol regulatory-element binding factor (*SREBF*)-1, carnitine palmitoyl transferase (*CPT*)-1 α , 3-hydroxy-3-methylglutaryl-coA reductase (*HMGCR*), fatty acid synthase (*FASN*), diacyl glycerol acyltransferase (*DGAT*) 1, *DGAT*2 and long/very long-chain acyl coA dehydrogenase (*ACADL*; *ACADLV*), peroxisome proliferator-activated receptor (*Ppar*) γ , acyl CoA dehydrogenase medium chain (*ACADM*).

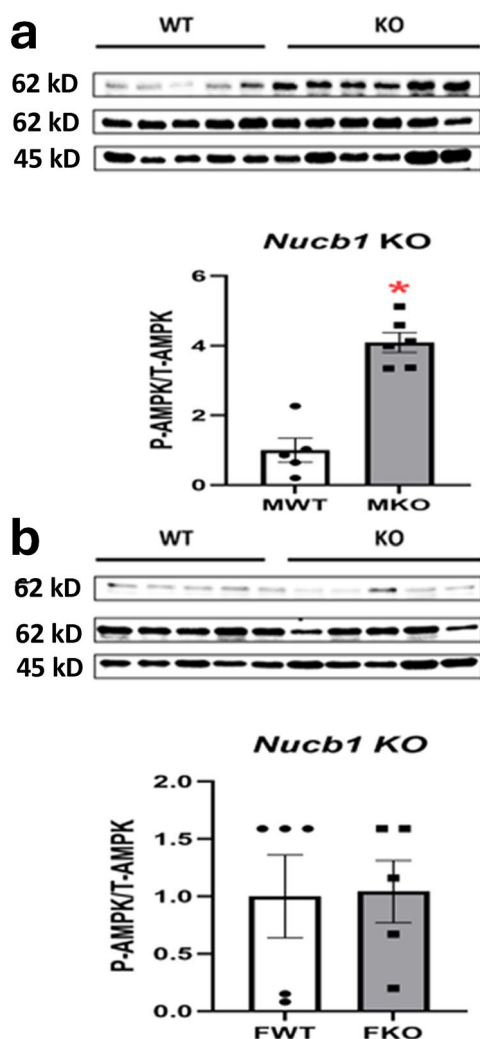


Fig. 8 | *NUCB1* disruption stimulated P-AMPK α /T-AMPK α ratio. The genetic disruption of nucleobindin 1 (*Nucb1*) increased the ratio of P-AMPK α /T-AMPK α in male mice liver (a), but not in female mice liver (b). The results presented are pooled from five liver samples per group. Asterisks show significant difference between knockout (KO) and wild-type (WT) groups. Significance was set at $P < 0.05$.

endogenous *Nucb* in male mice. Overall, the genetic disruption of *Nucb1* modulates hepatic lipid metabolism in a sex- and diet-specific manner.

In summary, our results provide the first scientific evidence supporting the direct regulation of hepatic lipid metabolism by NLP and NESF-1 through an AMPK-dependant manner in HepG2/C3A cells (Fig. 9). Genetic disruption of *Nucb1* gene affects lipid metabolism-related gene expression in a sex- and diet-specific manner. This report expands our understanding of NLP and NESF-1 as novel lipid-regulatory peptides in humans and rodents. The receptor that mediates NLP and NESF-1 action, the role of NLP on lipid metabolism in adipose tissue and studying the role of endogenous NUCB in hepatic lipid metabolism remain unknown. The outcome of our study set the stage to pursue a novel strategy targeting NUCB for addressing NAFLD. The results presented here also opens avenues for future research. For example, all studies here are conducted using a human liver cell line. The repetition of these experiments in human liver primary cells is one important next step. Additional studies to test whether nesfatin-1 and NLP affect metabolic fluxes and de novo lipogenesis as well as beta-oxidation fluxes warrant attention. In addition, in vivo studies to determine if the lipid-lowering effects, especially for NLP found in vitro exist in vivo in animal models of NAFLD.

Methods

Cell culture

Human hepatocellular carcinoma cells (HepG2/C3A cells, Catalog # CRL-1074, ATCC, USA) were grown as per protocol provided by the supplier, in 10 cm cell culture dish containing in 10 mL DMEM supplemented with 10% FBS at 37 °C in 5% CO₂ in 95% humidified atmosphere. HepG2/C3A cells are derived from HepG2 (ATCC HB-8065 is an epithelial-like cell isolated from the liver of a 15-year-old male patient with hepatocellular carcinoma. When cells reached the required confluency, they were used for specific experiments.

Immunocytochemistry

After seeding 1×10^8 cells/ 0.5 mL/well of four-well of chamber slides and cells reaching at 40% confluency, they were fixed by 4% paraformaldehyde (PFA) (Catalog # 158127, Sigma Canada) and washed with 1× PBS. Next, cells were incubated with a series of PBS-based solutions, including PBS-PF (Catalog # 1464510, Kodak, Canada), PBS-Triton X-100 (Catalog # 9036-19-5; Millipore Sigma Canada) and PBS-ABB (Pierce Catalog # 54200, Thermo Scientific, Canada), respectively. After incubation of cells with primary antibody overnight at 4 °C, they were incubated with secondary antibody at room temperature for 1 h and subsequently were washed with PBS-based solutions. Finally, chamber walls were removed, followed by the addition of Vectashield DAPI containing mounting medium (Catalog # H-1200-10, Vector Labs, California, USA) to cells, and then glass slides were applied to mount slides. All images were taken by Olympus DP70 camera and Olympus BX51 microscope (Olympus Canada, Toronto, Canada).

The primary antibodies used in this study were rabbit anti-mouse NUCB1 (1:200, custom synthesized, cat no. 1312-PAC-02, Pacific Immunology, USA), rabbit anti-mouse NUCB2 (1:200, RRID: AB_2891124, cat no. 1312-PAC-01, Pacific Immunology, USA). Secondary antibodies in this study were goat anti-rabbit Alexa Fluor 488 (1:200, RRID: AB_2630356, cat no. ab150077, ABCAM, UK). No primary antibody treated group was included as a negative control. Immunostaining obtained is referred to as NUCB1/NLP and NUCB2/NESF-1 to represent precursors and the encoded peptides detected by the primary antibodies used.

Induction of lipid accumulation in HepG2/C3A cells using OA

HepG2/C3A cells at approximately 60% confluency cultured in FBS-free medium (Thermo Scientific Canada) in four-well chamber slides were exposed to nontoxic concentration range of BSA conjugated-OA (O3008, Sigma-Aldrich®, Darmstadt, Germany) for 48 h and then lipid intensity area was measured by ORO staining. The concentration of OA and time point was chosen based on previous publications^{49,50}. The effective dose of OA was chosen based on ORO-based results.

Testing the effects of NLP and NESF-1 on lipid pathways-related enzymes mRNAs and endogenous *NUCB* and *NUCB* in untreated and OA-induced HepG2/C3A

HepG2/C3A cells at a confluency of 90% were incubated with 0.1 nM of mouse NLP (custom synthesized peptide, >95% purity, ABGENT, USA) or rat NESF-1 (cat no. 003-22B, Phoenix Pharmaceuticals Inc. CA, USA) for 24 h. The effective dose and time point were decided based on our pilot studies. To induce lipid accumulation, HepG2/C3A cells at a confluency of 50–60% were incubated with 0.5 mM BSA conjugated-OA for 48 h, then media refreshed with either rat NESF-1 or mouse NLP for another 24 h. Finally, RNA samples were extracted to assess the target transcript abundance by real-time quantitative PCR (qPCR). For OA-induced HepG2/C3A cell studies, quercetin (cat no. Q4951, Sigma-Aldrich, Darmstadt, Germany) was chosen as a positive control group. Quercetin doses were selected based on previous scientific findings⁵¹. Quercetin was dissolved in DMSO (Catalog # 136321-15-8; Millipore Sigma, Canada) as stock solution and then diluted in cell culture media (final concentration below 0.1%). The abundance of endogenous *NUCB* and *NUCB* levels was also assessed in OA-induced HepG2/C3A cells.

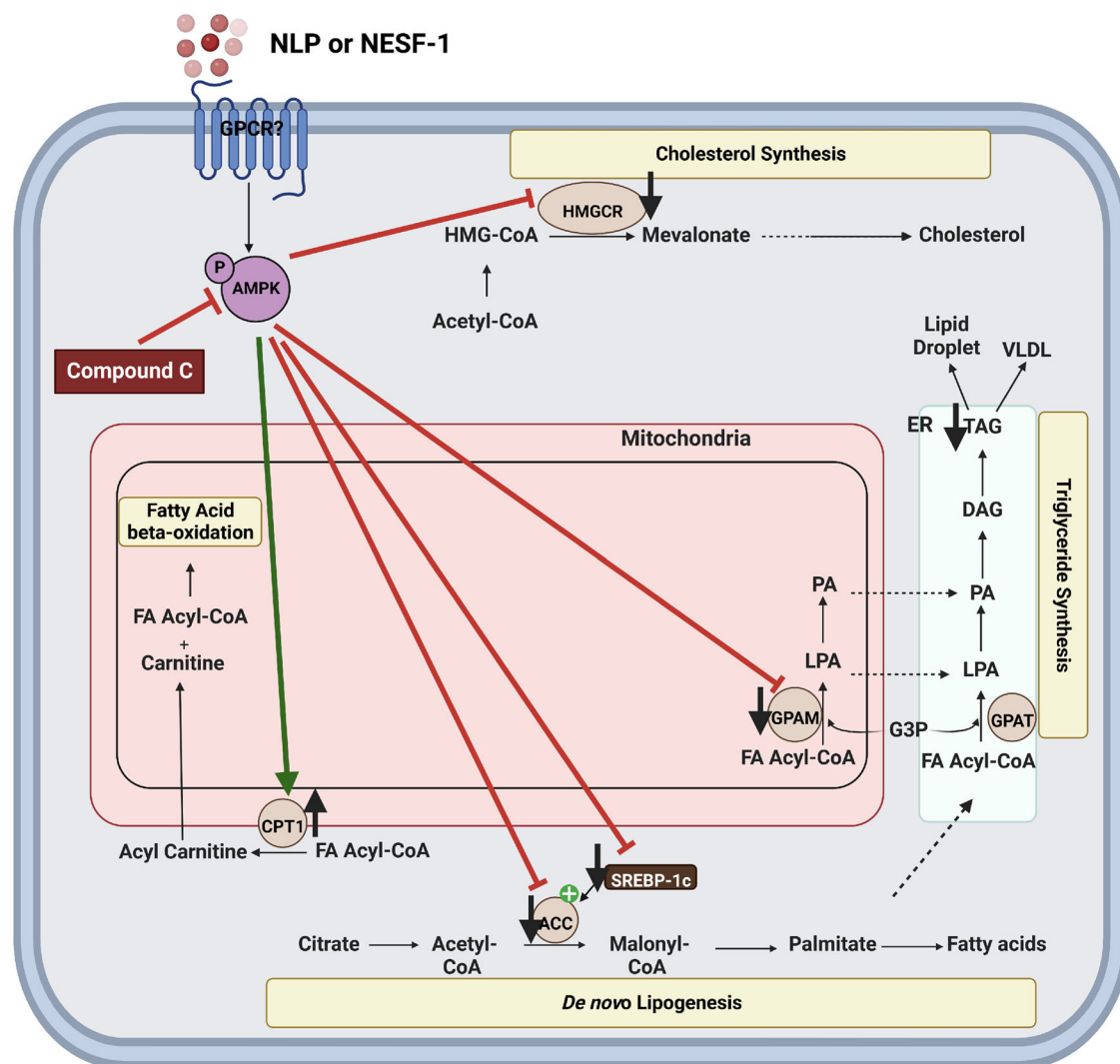


Fig. 9 | Scheme summarizing nesfatin-1 and NLP effects on hepatocyte lipid metabolism. This figure summarizes the effects of nesfatin-1 and NLP on hepatocyte lipid metabolism, detailed in this manuscript. Nesfatin-1 and NLP bind to a yet-to-be-characterized membrane-bound receptor and elicit their negative (suppressive) effects on cholesterol synthesis, triglyceride synthesis, and de novo lipogenesis. Meanwhile, both nesfatin-1 and NLP increased fatty acid oxidation enzyme mRNAs. Overall, both nesfatin-1 and NLP elicited a lowering of lipid levels. These actions are

mediated through the AMPK pathway. Enzymes shown are Acetyl-CoA carboxylase (*ACC*), glycerol-3-phosphate acyltransferase (*GPAM*), sterol regulatory-element binding factor (*SREBF*)-1, AMP kinase (*AMPK*), 3-hydroxy-3-methylglutaryl-coA reductase (*HMGCR*), and glycerol-3-phosphate acyltransferase (*GPAT*). This original figure was created using tools provided by Biorender, under a subscription purchased by the corresponding author.

ORO staining

A stock solution of 0.5% ORO (Allied Chemical, Morristown, NJ, USA) was prepared, and it was further diluted with sterile water (ratio 3:2) and filtered to make a working solution. OA-induced HepG2/C3A cells seeded in 4-well chamber slides at a confluency of 90% were incubated with an effective dose of rat NESF-1 or mouse NLP or quercetin for 24 h. No OA-treated controls (untreated groups) were also included in these studies. After fixing the cells in 4% paraformaldehyde (PFA), they were washed twice with 1× PBS. Chamber slide walls were removed, and slides were stained with ORO working solution for 15 min at room temperature. After rinsing with 60% isopropanol and subsequently in distilled water, they were mounted in glycerine jelly. Finally, sections were visualized using an Olympus BX51 microscope connected to an Olympus DP70 camera in light mode.

Mechanism of action of NLP and NESF-1 on HepG2 cells

A specific AMPK inhibitor, compound C (cat no. ab120843, ABCAM, UK) was used to block AMPK-mediated pathway in HepG2/C3A cells. Briefly, OA-induced cells at a confluency 90% were preincubated with compound C (10 μM) for 1 h, followed by incubation with peptides (0.1 nM) or quercetin

(10 μM), and compound C. Compound C stock was dissolved in DMSO and the level of DMSO in cell culture media was less than 0.1%. The concentration and time point for compound C incubation was chosen based on the recommended ranges found in the supplier catalog and were independently validated in pilot studies. Following the incubation, samples were collected for intracellular measurements as described below.

Measurement of cellular triglycerides

OA-induced HepG2/C3A cells were incubated with media containing the specified dose of peptides, positive control, and inhibitors in the six-well plate for 24 h, and then cells were used for lipid extraction using the hexane-isopropanol method with modifications^{52,53}. The groups consisted of media alone, NLP, NESF-1, quercetin, compound C, NLP + compound C, and NESF-1+compound C. Briefly, cells were washed with cold 1× PBS twice and then were scraped from the bottom of a six-well plate, followed by transferring into the new tubes. After centrifugation at 13,000 × g for 10 min, the supernatant was removed, and cell pellets were resuspended in hexane:isopropanol (3:2, v-v). This was followed by centrifugation using the same setup, and the supernatant was transferred to new tubes and dried at

50 °C overnight. Finally, dried viscous pellets were dissolved in isopropanol: NP-40 alternative (cat no. 492018, Sigma-Aldrich®, Darmstadt, Germany) (9:1, v- v) at 50 °C for 5 min. These samples were used to measure cellular TG content using Infinity TG liquid stable reagent (cat no. TR22421, Thermo Fisher Scientific, USA). For TG measurement, 3 µL of extracted samples were mixed with 300 µL of reagent per well of a 96-well plate at 37 °C for 5 min, and then the absorbance of each well was measured in primary and secondary wavelengths of 500 and 660 nm using a Varioskan LUX multimode microplate reader (Thermo Fisher Scientific, USA). TGs were calculated based on the formula mentioned in the instruction of the reagent as mentioned below:

$$\text{TGs (mmol/L)} = (\text{absorbance of unknown}) / (\text{absorbance of calibrator}) \times \text{calibrator value.}$$

Animals

To characterize the effects of the genetic disruption of *Nucb1* in the lipid metabolism, breeding pairs of homozygous C57BL/6N^{Crl-Nucb1em1(IMPC)Mbp/Mmucd} mice from the University of California, San Diego (generated by Dr. Kent Lloyd, Mouse Biology Program, University of California-Davis, USA) were used to establish a colony of *Nucb1*-disrupted mice. To generate these global *Nucb1*-disrupted mice, the exon 4 and flanking splicing regions of *Nucb1* were constitutively deleted using CRISPR Cas9 gene editing technology in C57BL/6 J mouse zygotes. Further details on the phenotype of this strain of mice are furnished in ref. 54.

All animals were housed under 12 h light:12 h dark cycle (7 am–7 pm), humidity (30–60%), and temperature (18–22 °C) controlled vivarium located in the Western College of Veterinary Medicine Animal Care Unit, University of Saskatchewan. All *Nucb1* KO mice studies followed the guidelines of the Canadian Council for Animal Care and were approved by the University of Saskatchewan Animal Care Committee (2012-0033). Age-matched mice were chosen and fed a control fat diet (Cat no. D12450B, Research Diets Inc., 70% carbohydrate, 20% protein, 10% fat, Energy density = 3.82 Kcal/g) and high-fat diet (cat no. D12492, Research Diets Inc., 20% carbohydrate, 20% protein, 60% fat, Energy density = 5.21 Kcal/g) for 6 months. Liver samples from these mice were collected after cervical dislocation, total RNA was extracted, and the expression of liver genes was assessed.

RNA extraction, cDNA synthesis, and RT-qPCR

The above procedures were carried out as described in our previously reported protocols²¹. Briefly, RNA was extracted using Ribozol (cat no. N580, VWR, USA), and then RNA's quantity and quality were determined by NanoDrop 2000 (Thermo Fisher Scientific). The RNA was reverse transcribed to the cDNA using iScript Reverse Transcription Supermix for RT-qPCR (cat no. 170884, Bio-Rad, USA) followed by the quantitative measurement of mRNA expression by qPCR in a CFX Connect Optic module (Bio-Rad, USA) following the requirements of the MIQE guidelines⁵⁵ and using SensiFAST™ SYBR No-ROX MIX (cat no. BIO-98050, Biorline, UK). The primers sequence and annealing temperature are listed in Table S1 (Supplementary Table 1) purchased from Integrated DNA Technologies (IDT). Three negative controls, including no template DNA (NTC control), no reverse transcriptase control from cDNA synthesis process (RTC control), and a nuclease-free water sample (PCR control), were also included for each gene expression study. Thermal cycling setup for all genes was the following: denaturation (95 °C for 5 s), annealing (specific for each primer for 25 s) and elongation (60 °C for 25 s), 35 cycles. At least three independent experiments with triplicates for in vitro studies (final samples ≥9) and more than five mice/group/sex were considered. The abundance of mRNA was calculated based on the Pfaffl method and gene-specific efficiencies⁵⁶, relative to the geometric means of the 2 housekeeping genes. Four different housekeeping genes (Beta actin, GAPDH, HMBS, and HMBeta2) were tested in HepG2 cell studies. HMBS and HMBeta2 for

HepG2 cell studies had constant Ct values and better stability values, and they were chosen as internal controls.

Western blot analysis

The analysis of protein expression was done according to the previously reported protocols²¹. Briefly, total protein was extracted using RIPA Lysis, and Extraction Buffer (cat no. 89901, Thermo Fisher Scientific, USA) and the concentration of protein was determined by Bradford assay. Then, 35 µg of crude protein was electrophoresed on 8–16% Mini-Protean TGX gels (cat no. 456-1104, Bio-Rad, USA), and the protein bands were transferred to nitrocellulose membranes (cat no. 1704158, Bio-Rad, USA) using the Trans-Blot Turbo Transfer System (Bio-Rad, USA). After blocking the membrane with rapid blocking buffer 1× (cat no. M325, VWR, USA) for 15 min at room temperature, it was incubated with primary antibodies overnight at 4 °C followed by washing with TBST (0.1% Tween-20 in TBS) thrice for 15 min each time. In the next step, nitrocellulose membranes were incubated with a secondary antibody for 1 h at 37 °C, and final washing steps were completed. The membranes were visualized using a ChemiDoc MP Imaging System (Bio-Rad, USA). The band intensity was analyzed by ImageJ (National Institutes of Health, Bethesda, MD, USA). All blot images are provided as Supplementary Figs. 2–5.

Primary antibodies used in this study were monoclonal mouse anti-beta-actin antibody (1:1000, RRID: AB_528068, cat no. JLA20, Developmental Studies Hybridoma Bank, DSHB, University of Iowa, USA), rabbit anti-mouse NUCB1 (1:250, custom synthesized, cat no. 1312-PAC-02, Pacific Immunology, USA), rabbit anti-mouse NUCB2 (1:250, RRID: AB_2891124, cat no. 1312-PAC-01, Pacific Immunology, USA), polyclonal rabbit anti-phospho (Thr172)-AMPKα antibody (1:1000, RRID: AB_330330, cat no. 2531S, Cell Signalling, USA), polyclonal rabbit anti-AMPKα antibody (1:1000, RRID: AB_330331, cat no. 2532S, Cell Signalling, USA). The secondary antibodies used were goat anti-rabbit IgG (H + L)-HRP conjugate antibody (1:5000, RRID: AB_11125142, cat no. 170-6515, Bio-Rad, USA) and goat anti-mouse IgG (H + L)-HRP conjugate antibody (1: 5000, RRID: AB_11125547, cat no. 170-6516, Bio-Rad, USA).

Statistical analysis

All values are shown as mean ± SEM. Statistical analysis was conducted by SPSS statistical software (IBM SPSS Statistics for Windows, Version 23.0, USA). The normality of data and the presence of outliers were assessed by Shapiro–Wilk's test and drawing box plot, respectively. The homogeneity of variances was analyzed by Leven's test. The single comparison was performed by Student's *t* test. Multiple comparisons were done by one-way ANOVA followed by Tukey's multiple comparison test. The three-way ANOVA was performed to evaluate the main effect or combination of three independent variables (diet, sex, gene disruption) on response variables (lipogenic or beta-oxidation gene expression) in mice. The significance level was set at *P* < 0.05. Graphs were plotted by GraphPad Prism (GraphPad Software, Inc., Prism 8 for Windows, Version 8.4.2, USA).

Reporting summary

Further information on research design is available in the Nature Portfolio Reporting Summary linked to this article.

Data availability

Extra information supporting the findings of this study and primer sequences are available within its supplementary information file. The raw data that support the findings of this study are provided as Supplementary Data 1 in MS Excel format.

Received: 16 February 2023; Accepted: 9 May 2024;

Published online: 27 May 2024

References

- Kawano, J.-i et al. CALNUC (nucleobindin) is localized in the Golgi apparatus in insect cells. *Eur. J. Cell Biol.* **79**, 208–217 (2000).
- Wang, S. N. et al. Antigen expression associated with lymph node metastasis in gastric adenocarcinomas. *Pathol. Int.* **44**, 844–849 (1994).
- Lavoie, C., Meerloo, T., Lin, P. & Farquhar, M. G. Calnuc, an EF-hand Ca²⁺-binding protein, is stored and processed in the Golgi and secreted by the constitutive-like pathway in AtT20 cells. *Mol. Endocrinol.* **16**, 2462–2474 (2002).
- Kanuru, M., Raman, R. & Aradhyam, G. K. Serine protease activity of calnuc: regulation by Zn²⁺ and G proteins. *J. Biol. Chem.* **288**, 1762–1773 (2013).
- Oh-I, S. et al. Identification of nesfatin-1 as a satiety molecule in the hypothalamus. *Nature* **443**, 709–712 (2006).
- Yosten, G., Redlinger, L. & Samson, W. Evidence for a role of endogenous nesfatin-1 in the control of water drinking. *J. Neuroendocrinol.* **24**, 1078–1084 (2012).
- Yin, Y. et al. AMPK-dependent modulation of hepatic lipid metabolism by nesfatin-1. *Mol. Cell. Endocrinol.* **417**, 20–26 (2015).
- Foo, K. S., Brauner, H., Östenson, C.-G. & Broberger, C. Nucleobindin-2/nesfatin in the endocrine pancreas: distribution and relationship to glycaemic state. *J. Endocrinol.* **204**, 255 (2010).
- Gonzalez, R. et al. Nutrient responsive nesfatin-1 regulates energy balance and induces glucose-stimulated insulin secretion in rats. *Endocrinology* **152**, 3628–3637 (2011).
- Gonzalez, R. et al. Nesfatin-1 regulates the hypothalamo-pituitary-ovarian axis of fish. *Biol. Reprod.* **87**, 81–11 (2012).
- Vas, S. et al. Nesfatin-1/NUCB2 as a potential new element of sleep regulation in rats. *PLoS ONE* **8**, e59809 (2013).
- Foo, K., Brismar, H. & Broberger, C. Distribution and neuropeptide coexistence of nucleobindin-2 mRNA/nesfatin-like immunoreactivity in the rat CNS. *Neuroscience* **156**, 563–579 (2008).
- Stengel, A. et al. Identification and characterization of nesfatin-1 immunoreactivity in endocrine cell types of the rat gastric oxyntic mucosa. *Endocrinology* **150**, 232–238 (2009).
- Zhang, A.-Q. et al. Expression of nesfatin-1/NUCB2 in rodent digestive system. *World J. Gastroenterology: WJG* **16**, 1735 (2010).
- Tagaya, Y. et al. Secreted nucleobindin-2 inhibits 3T3-L1 adipocyte differentiation. *Protein Pept. Lett.* **19**, 997–1004 (2012).
- Tagaya, Y., Miura, A., Okada, S., Ohshima, K. & Mori, M. Nucleobindin-2 is a positive modulator of EGF-dependent signals leading to enhancement of cell growth and suppression of adipocyte differentiation. *Endocrinology* **153**, 3308–3319 (2012).
- Başar, Ö. et al. A novel appetite peptide, nesfatin-1 in patients with non-alcoholic fatty liver disease. *Scand. J. Clin. Lab. Investig.* **72**, 479–483 (2012).
- Tulke, S. et al. Nucleobindin 1 (NUCB1) is a Golgi-resident marker of neurons. *Neuroscience* **314**, 179–188 (2016).
- Ramesh, N., Mohan, H. & Unniappan, S. Nucleobindin-1 encodes a nesfatin-1-like peptide that stimulates insulin secretion. *Gen. Comp. Endocrinol.* **216**, 182–189 (2015).
- Sundarrajan, L. et al. Nesfatin-1-like peptide encoded in nucleobindin-1 in goldfish is a novel anorexigen modulated by sex steroids, macronutrients and daily rhythm. *Sci. Rep.* **6**, 1–14 (2016).
- Nasri, A. & Unniappan, S. Nucleobindin-derived nesfatin-1 and nesfatin-1-like peptide stimulate pro-opiomelanocortin synthesis in murine AtT-20 corticotrophs through the cAMP/PKA/CREB signaling pathway. *Mol. Cell. Endocrinol.* **536**, 111401 (2021).
- Garcia, D. & Shaw, R. J. AMPK: mechanisms of cellular energy sensing and restoration of metabolic balance. *Mol. Cell* **66**, 789–800 (2017).
- Gnoni, A. et al. Quercetin reduces lipid accumulation in a cell model of NAFLD by inhibiting de novo fatty acid synthesis through the acetyl-CoA carboxylase 1/AMPK/PP2A axis. *Int. J. Mol. Sci.* **23**, 1044 (2022).
- Vélez, E. J. & Unniappan, S. Nesfatin-1 and nesfatin-1-like peptide suppress growth hormone synthesis via the AC/PKA/CREB pathway in mammalian somatotrophs. *Sci. Rep.* **10**, 1–12 (2020).
- Williams, P., Tulke, S., Illegems, E., Berggren, P.-O. & Broberger, C. Expression of nucleobindin 1 (NUCB1) in pancreatic islets and other endocrine tissues. *Cell Tissue Res.* **358**, 331–342 (2014).
- Goebel-Stengel, M., Wang, L., Stengel, A. & Taché, Y. Localization of nesfatin-1 neurons in the mouse brain and functional implication. *Brain Res.* **1396**, 20–34 (2011).
- Goebel-Stengel, M. & Wang, L. Central and peripheral expression and distribution of NUCB2/nesfatin-1. *Curr. Pharm. Des.* **19**, 6935–6940 (2013).
- Hui, J., Aulakh, G. K., Unniappan, S. & Singh, B. Loss of Nucleobindin-2/Nesfatin-1 increases lipopolysaccharide-induced murine acute lung inflammation. *Cell Tissue Res.* **385**, 87–103 (2021).
- Stengel, A. et al. Ghrelin and NUCB2/nesfatin-1 are expressed in the same gastric cell and differentially correlated with body mass index in obese subjects. *Histochem. Cell Biol.* **139**, 909–918 (2013).
- Garcia-Galiano, D. et al. Cellular distribution, regulated expression, and functional role of the anorexigenic peptide, NUCB2/nesfatin-1, in the testis. *Endocrinology* **153**, 1959–1971 (2012).
- Sun, D. & Yang, H. Tissue-specific localization NUCB2/nesfatin-1 in the liver and heart of mouse fetus. *Dev. Reprod.* **22**, 331–339 (2018).
- Blanco, A. M. et al. Nesfatin-1 is an inhibitor of the growth hormone-insulin-like growth factor axis in goldfish (*Carassius auratus*). *J. Neuroendocrinol.* **33**, e13010 (2021).
- Wang, Y. et al. Nesfatin-1 promotes brown adipocyte phenotype. *Sci. Rep.* **6**, 1–10 (2016).
- Blanco, A. M., Velasco, C., Bertucci, J. I., Soengas, J. L. & Unniappan, S. Nesfatin-1 regulates feeding, glucosensing and lipid metabolism in rainbow trout. *Front. Endocrinol.* **9**, 484 (2018).
- Li, X. et al. Quercetin improves insulin resistance and hepatic lipid accumulation in vitro in a NAFLD cell model. *Biomed. Rep.* **1**, 71–76 (2013).
- Ramirez-Zacarias, J., Castro-Munozledo, F. & Kuri-Harcuch, W. Quantitation of adipose conversion and triglycerides by staining intracytoplasmic lipids with Oil Red O. *Histochemistry* **97**, 493–497 (1992).
- Kawano, Y. & Cohen, D. E. Mechanisms of hepatic triglyceride accumulation in non-alcoholic fatty liver disease. *J. Gastroenterol.* **48**, 434–441 (2013).
- Chen, X. X. et al. Resveratrol reduces glucolipid metabolic dysfunction and learning and memory impairment in a NAFLD rat model: involvement in regulating the imbalance of Nesfatin-1 abundance and copine 6 expression. *Front. Endocrinol.* **10**, 434 (2019).
- Brailoiu, G. C. et al. Nesfatin-1: distribution and interaction with a G protein-coupled receptor in the rat brain. *Endocrinology* **148**, 5088–5094 (2007).
- Osei-Hyiaman, D., Di, S., Nishimura, S. & Encinas, J. Fasting co-suppresses Nesfatin-1 and GPR12 in mouse hypothalamic appetite center: implications for energy metabolism. *Endocr. Rev.* **32**, 2–300 (2011).
- Dzamko, N. et al. AMPK β 1 deletion reduces appetite, preventing obesity and hepatic insulin resistance. *J. Biol. Chem.* **285**, 115–122 (2010).
- Jelenik, T. et al. AMP-activated protein kinase α 2 subunit is required for the preservation of hepatic insulin sensitivity by n-3 polyunsaturated fatty acids. *Diabetes* **59**, 2737–2746 (2010).
- Yang, M. et al. Nesfatin-1 action in the brain increases insulin sensitivity through Akt/AMPK/TORC2 pathway in diet-induced insulin resistance. *Diabetes* **61**, 1959–1968 (2012).
- Liu, Y. et al. Central nesfatin-1 activates lipid mobilization in adipose tissue and fatty acid oxidation in muscle via the sympathetic nervous system. *BioFactors* **46**, 454–464 (2020).
- Peng, J. et al. Quercetin improves glucose and lipid metabolism of diabetic rats: involvement of Akt signaling and SIRT1. *J. Diabetes Res.* **2017**, 3417306 (2017).

46. Zeng, H. et al. Quercetin alleviates ethanol-induced liver steatosis associated with improvement of lipophagy. *Food Chem. Toxicol.* **125**, 21–28 (2019).
47. de Conti, A. et al. Characterization of the variability in the extent of non-alcoholic fatty liver induced by a high-fat diet in the genetically diverse Collaborative Cross mouse model. *FASEB J.* **34**, 7773 (2020).
48. Lorbek, G., Perše, M., Horvat, S., Björkhem, I. & Rozman, D. Sex differences in the hepatic cholesterol sensing mechanisms in mice. *Molecules* **18**, 11067–11085 (2013).
49. Cui, W., Chen, S. L. & Hu, K.-Q. Quantification and mechanisms of oleic acid-induced steatosis in HepG2 cells. *Am. J. Transl. Res.* **2**, 95 (2010).
50. Guo, L. et al. S-petasin inhibits lipid accumulation in oleic acid-induced HepG2 cells through activation of the AMPK signaling pathway. *Food Funct.* **11**, 5664–5673 (2020).
51. Chen, L. et al. Quercetin and non-alcoholic fatty liver disease: a review based on experimental data and bioinformatic analysis. *Food Chem. Toxicol.* **154**, 112314 (2021).
52. Hara, A. & Radin, N. S. Lipid extraction of tissues with a low-toxicity solvent. *Anal. Biochem.* **90**, 420–426 (1978).
53. Zhang, R. et al. Myeloperoxidase functions as a major enzymatic catalyst for initiation of lipid peroxidation at sites of inflammation. *J. Biol. Chem.* **277**, 46116–46122 (2002).
54. Nasri, A. et al. Nucleobindin-1 (Nucb1) disruption affects feeding, metabolism, and glucose homeostasis in mice in an age-, sex-, diet- and light cycle-dependent manner. Preprint at <https://www.biorxiv.org/content/10.1101/2024.03.07.584005v1> (2024).
55. Bustin, S. A. et al. *The MIQE Guidelines: Minimum Information for Publication of Quantitative Real-Time PCR Experiments* (Oxford University Press, 2009).
56. Pfaffl, M. W. A new mathematical model for relative quantification in real-time RT-PCR. *Nucleic Acids Res.* **29**, e45–e45 (2001).

Acknowledgements

This research was partly supported by the Canadian Institutes of Health Research (CIHR) and the University of Saskatchewan Centennial Enhancement Chair in Comparative Endocrinology to S.U. Infrastructure support for the project was provided by John Evans Leader's Fund grant from the Canada Foundation of Innovation (CFI) and an Establishment Grant from the Saskatchewan Foundation of Health Research (SHRF) to S.U. A.N. was supported by a Dean's scholarship from the University of Saskatchewan.

Author contributions

A.N. and M.K. were responsible for conducting the experiments, and A.N. was responsible for data analyses and writing the first draft of the manuscript. S.B.W. provided insights on hepatocyte studies and interpretation of the data, as well as some reagents critical for the in vitro studies and provided feedback on the manuscript. S.U. was responsible for original ideas, funding, study planning, work management, and manuscript editing and submission.

Competing interests

The authors declare no competing interests.

Additional information

Supplementary information The online version contains supplementary material available at <https://doi.org/10.1038/s42003-024-06314-2>.

Correspondence and requests for materials should be addressed to Suraj Unniappan.

Peer review information *Communications Biology* thanks the anonymous reviewers for their contribution to the peer review of this work. Primary Handling Editors: Jesmond Dalli and Joao Valente.

Reprints and permissions information is available at <http://www.nature.com/reprints>

Publisher's note Springer Nature remains neutral with regard to jurisdictional claims in published maps and institutional affiliations.

Open Access This article is licensed under a Creative Commons Attribution 4.0 International License, which permits use, sharing, adaptation, distribution and reproduction in any medium or format, as long as you give appropriate credit to the original author(s) and the source, provide a link to the Creative Commons licence, and indicate if changes were made. The images or other third party material in this article are included in the article's Creative Commons licence, unless indicated otherwise in a credit line to the material. If material is not included in the article's Creative Commons licence and your intended use is not permitted by statutory regulation or exceeds the permitted use, you will need to obtain permission directly from the copyright holder. To view a copy of this licence, visit <http://creativecommons.org/licenses/by/4.0/>.

© The Author(s) 2024